J. Fluid Mech. (1975), *vol.* 68, *part* 2, *pp.* 321–343
Printed in Great Britain

Buoyancy effects in a horizontal flat-plate boundary layer

By S. P. S. ARYA
Department of Atmospheric Sciences, University of Washington, Seattle

(Received 20 May 1974)

Observations made in a well-developed, thermally stratified, horizontal, flat-plate boundary layer are used to study the effects of buoyancy on the mean flow and turbulence structure. These are represented in a similarity framework obtained from the concept of local equilibrium in a fully developed turbulent flow. Mean velocity and temperature profiles in both the inner and outer layers are strongly dependent on the thermal stratification, the former suggesting an increase in the thickness of the viscous sublayer with increasing stability. The coefficients of skin friction and heat transfer, on the other hand, decrease with increasing stability.

Normalized turbulent intensities, fluxes and their correlation coefficients also vary with buoyancy. In stable conditions, turbulence becomes rapidly suppressed with increasing stability as more and more energy has to be expended in overcoming buoyancy forces. The buoyancy effects are found to be more dominant in the stress budget than in the turbulent energy budget. The horizontal heat flux is much greater than the vertical heat flux and their ratio increases with stability. The ratio of the eddy diffusivities of heat and momentum, on the other hand, decreases with increasing stability. The spectra of velocity and temperature fluctuations indicate no buoyancy subrange, but the wavenumber corresponding to peak energy is found to increase with increasing stability.

1. Introduction

Density-stratified boundary layers in which buoyancy plays an important role in turbulent transfer often occur in nature, and have been extensively studied by meteorologists and oceanographers (Monin & Yaglom 1971; Kraus 1972; Turner 1973). The feasibility of their simulation in the laboratory has, in recent years, also led to their study in specially designed wind tunnels and other facilities (Ellison & Turner 1960; Cermak *et al.* 1966; Deardorff & Willis 1967; Arya & Plate 1969*a*, *b*; Nicholl 1970; Mery, Schon & Solal 1974).

In the engineering heat-transfer literature, buoyancy effects have been considered only with reference to natural convection or mixed convection boundary layers developing over vertical or inclined plates. For horizontal boundary layers, temperature is usually considered to be a passive scalar and heating is assumed not to have any dynamical effects. In most experiments such conditions are indeed realized. With increasing thermal stratification, however, buoyancy

effects on the mean flow and turbulence structure could become significant and even dominant. In gas flows, a simple measure of thermal stratification is given by a bulk Richardson number

$$Ri_\delta = \frac{g\delta\,\overline{\Theta}_\infty}{T_0\,\overline{U}_\infty^2}, \tag{1}$$

where $\overline{\Theta}_\infty$ is the potential temperature difference across the boundary layer, whose thickness is δ and ambient velocity $\overline{U}_\infty$, g is the acceleration due to gravity and T_0 is the average absolute temperature of the layer. In more general cases, where stratification may occur owing to causes other than heating, a bulk Richardson number can be similarly defined in terms of density differences across the layer and the coefficient of expansion of the fluid (Ellison & Turner 1960).

Nicholl (1970) has studied the dynamical effects of heat in a horizontal flat-plate boundary layer (see also Townsend 1958). His experiments were carried out in a relatively small wind tunnel and, consequently, his interesting results are more typical of a rapidly developing, non-equilibrium transition layer immediately following a large temperature discontinuity than of a well-developed equilibrium boundary layer far downstream from the discontinuity. The latter situation has been investigated by the present author in his doctoral dissertation (Arya 1968); important results of this and some later experimental work will be reported here. Since a suitable framework for presenting and discussing observations is provided by some theoretical and similarity ideas, these are discussed first.

2. Theoretical and similarity considerations

Dynamical equations and theoretical models

From the equations of motion of a stratified fluid, using the Boussinesq approximation and Reynolds averaging technique, one obtains the equations of mean motion (Lumley & Panofsky 1964, p. 63):

$$\frac{\partial \overline{U}_i}{\partial t} + \overline{U}_j \frac{\partial \overline{U}_i}{\partial x_j} = -\frac{1}{\rho_0}\frac{\partial \overline{P}}{\partial x_i} + \frac{\partial}{\partial x_j}\left(\nu \frac{\partial \overline{U}_i}{\partial x_j} - \overline{u_i u_j}\right) - \frac{g}{T_0}\overline{\Theta}\,\delta_{3i}, \tag{2}$$

$$\partial \overline{U}_j / \partial x_j = 0, \tag{3}$$

$$\frac{\partial \overline{\Theta}}{\partial t} + \overline{U}_j \frac{\partial \overline{\Theta}}{\partial x_j} = \frac{\partial}{\partial x_j}\left(k \frac{\partial \overline{\Theta}}{\partial x_j} - \overline{\theta u_j}\right), \tag{4}$$

where t denotes time, the x_1 axis is taken in the direction of the mean flow, with x_2 in the lateral and x_3 in the vertical direction, the $\overline{U}_i$ and u_i ($i = 1, 2, 3$) are the components of the mean and fluctuating velocity, respectively, $\overline{\Theta}$ and θ are the mean and fluctuating temperature, $\overline{P}$ and p the mean and fluctuating pressure, ρ_0 the density, ν the kinematic viscosity, k the thermal diffusivity and δ_{ij} is Kronecker's delta function.

Similarly, from the equations for the fluctuating components of the velocity and temperature one can obtain a hierarchy of dynamical equations relating the

various statistics of turbulence (see, for example, Monin & Yaglom 1971, p. 377). Of special interest to us are the equations of second moments:

$$\frac{1}{2}\frac{\partial \overline{u_\alpha u_\alpha}}{\partial t}+\tfrac{1}{2}\overline{U}_j\frac{\partial \overline{u_\alpha u_\alpha}}{\partial x_j}+\frac{1}{2}\frac{\partial \overline{u_\alpha u_\alpha u_j}}{\partial x_j}=-\overline{u_\alpha u_j}\frac{\partial \overline{U}_\alpha}{\partial x_j}+\frac{g}{T_0}\overline{u_\alpha\theta}\,\delta_{3\alpha}-\frac{1}{\rho_0}\overline{u_\alpha\frac{\partial p}{\partial x_\alpha}}-\nu\overline{\frac{\partial u_\alpha}{\partial x_j}\frac{\partial u_\alpha}{\partial x_j}}, \tag{5}$$

$$\frac{1}{2}\frac{\partial \overline{\theta\theta}}{\partial t}+\tfrac{1}{2}\overline{U}_j\frac{\partial \overline{\theta\theta}}{\partial x_j}+\frac{1}{2}\frac{\partial \overline{\theta\theta u_j}}{\partial x_j}=-\overline{u_j\theta}\frac{\partial \overline{\Theta}}{\partial x_j}-k\overline{\frac{\partial\theta}{\partial x_j}\frac{\partial\theta}{\partial x_j}}, \tag{6}$$

$$\begin{aligned}&\frac{\partial \overline{u_iu_k}}{\partial t}+\overline{U}_j\frac{\partial \overline{u_iu_k}}{\partial x_j}+\frac{\partial \overline{u_iu_ku_j}}{\partial x_j}\\&\quad=-\overline{u_iu_j}\frac{\partial \overline{U}_k}{\partial x_j}-\overline{u_ku_j}\frac{\partial \overline{U}_i}{\partial x_j}+\frac{g}{T_0}(\overline{u_i\theta}\,\delta_{3k}+\overline{u_k\theta}\,\delta_{3i})-\frac{1}{\rho_0}\left(\overline{u_k\frac{\partial p}{\partial x_i}}+\overline{u_i\frac{\partial p}{\partial x_k}}\right)-2\nu\overline{\frac{\partial u_i}{\partial x_j}\frac{\partial u_k}{\partial x_j}},\end{aligned} \tag{7}$$

$$\frac{\partial \overline{u_i\theta}}{\partial t}+\overline{U}_j\frac{\partial \overline{u_i\theta}}{\partial x_j}+\frac{\partial \overline{\theta u_iu_j}}{\partial x_j}=-\overline{u_j\theta}\frac{\partial \overline{U}_i}{\partial x_j}-\overline{u_iu_j}\frac{\partial \overline{\Theta}}{\partial x_j}+\frac{g}{T_0}\overline{\theta\theta}\,\delta_{3i}-\frac{1}{\rho_0}\overline{\theta\frac{\partial p}{\partial x_i}}-(\nu+k)\overline{\frac{\partial\theta}{\partial x_j}\frac{\partial u_i}{\partial x_j}}. \tag{8}$$

Here, we have omitted the molecular diffusion terms, which will be significant only very close to the wall (in the viscous sublayer region). If we use the convention that a repeated Greek index does not mean summation, equations (5) represent the budgets of component energies, (6) the budgets of mean-square temperature fluctuations and (7) and (8) the budgets of turbulent momentum and heat fluxes respectively.

In (5)–(8), the first term on the left-hand side represents the time rate of change of the particular turbulent quantity and is zero in a steady flow; the second term represents advection or transport by the mean flow and would be zero in a horizontally homogeneous flow; the third term represents turbulent diffusion, whose integral over the whole boundary layer should be zero. Locally, diffusion terms may be quite significant, especially in the outer region of the boundary layer; the mere presence of these higher-order terms constitutes the fundamental closure problem for the dynamical equations of any turbulent flow. On the right-hand sides of (5)–(8), the terms containing gradients of mean velocity and temperature represent mechanical production, and those containing the buoyancy variable g/T_0 represent buoyant production or destruction (depending upon whether the stratification is unstable or stable). The terms representing correlations of velocity or temperature fluctuations with the gradients of pressure fluctuations are referred to as pressure strain or 'return to isotropy' terms; they act as sinks for all quantities characterizing anisotropy in a turbulent flow. Finally, the last terms containing molecular diffusivities are the so-called dissipation terms, which are quite important in the budgets of turbulent energies and mean-square temperature fluctuations, but are generally insignificant, in the limit of large Reynolds number, in the budgets of momentum and heat fluxes (see, for example, Wyngaard, Coté & Izumi 1971).

The theoretical models proposed by Ellison (1957) and Townsend (1958) are based on the equations for the turbulent energy and mean-square temperature

fluctuations (Ellison used the equation for the vertical heat flux also), with some *ad hoc* and very rough closure assumptions (see Arya 1972*a*). More sophisticated models of the horizontally homogeneous, stratified boundary layer have since then been proposed by Monin (1965), Mellor (1973), Lewellen & Teske (1973) and Wyngaard, Coté & Rao (1974). These are all based on the second-moment equations (5)–(8) with different closure assumptions. The original Navier–Stokes equations have been integrated numerically by Deardorff (1972) for the unstable atmospheric boundary layer.

Similarity considerations

The concept of local similarity (Clauser 1956; Brundrett & Burroughs 1967; Kader & Yaglom 1972) suggests that in the boundary layer far downstream of a temperature discontinuity all the mean flow and turbulent characteristics at a certain location must depend only on the following local variables:

$$z, \quad \overline{U}_\infty, \quad \overline{\Theta}_\infty, \quad \delta, \quad \delta_\theta, \quad \nu, \quad k, \quad g/T_0, \tag{9}$$

where δ_θ is thermal boundary-layer thickness. Then, from dimensional analysis, quantities like $\overline{U}/\overline{U}_\infty$, $\overline{\Theta}/\overline{\Theta}_\infty$, $\overline{u^2}/\overline{U}_\infty^2$, $\overline{v^2}/\overline{U}_\infty^2$, $\overline{w^2}/\overline{U}_\infty^2$, $\overline{\theta^2}/\overline{\Theta}_\infty^2$, $\overline{uw}/\overline{U}_\infty^2$, $\overline{w\theta}/\overline{U}_\infty\overline{\Theta}_\infty$, $\overline{u\theta}/\overline{U}_\infty\overline{\Theta}_\infty$, etc., must be universal functions of the following dimensionless parameters:

$$z/\delta, \quad Re_\delta, \quad Ri_\delta, \quad Pr, \quad \delta_\theta/\delta, \tag{10}$$

where $Re_\delta = \overline{U}_\infty\delta/\nu$ is Reynolds number, $Pr = \nu/k$ is Prandtl number and Ri_δ is the bulk Richardson number defined in (1). Since we are mainly concerned with the flow of air, Pr is dropped from further consideration. In a well-developed boundary layer, the ratio δ_θ/δ is expected to be close to unity and is also not important.

The so-called universal law of wall similarity (Hinze 1959, p. 466) is based on the observation that the external variables $\overline{U}_\infty$, $\overline{\Theta}_\infty$, δ, etc., are not directly relevant to the similarity of flow in the wall region or surface layer, if the velocity and temperature are scaled by $u_* = (\tau_0/\rho_0)^{\frac{1}{2}}$ and $\theta_* = -Q_0/u_*$, where τ_0 is the shear stress and Q_0 the kinematic heat flux at the surface. An extension of this to stratified conditions was originally proposed by Monin & Oboukhov (1954); their similarity hypothesis introduces a stability parameter

$$\zeta = -zkgQ_0/T_0u_*^3, \tag{11}$$

on which all the properly scaled mean flow and turbulent quantities must depend. This type of similarity has been roughly demonstrated by atmospheric observations (Zilitinkevich & Chalikov 1968; Businger *et al.* 1971; Wyngaard, Coté & Isumi 1971), and also by some wind-tunnel observations (Arya & Plate 1969*b*; Mery, Schon & Solal 1974).

The asymptotic matching of the inner- and outer-layer similarity profiles of mean velocity and temperature leads to the following 'universal' drag and heat-transfer relations for an unstratified constant-pressure boundary layer over a smooth flat plate (Clauser 1956; Brundrett & Burroughs 1967; Kader & Yaglom 1972):

$$\frac{\overline{U}_\infty}{u_*} = \frac{1}{k}\left[\ln\frac{u_*\delta}{\nu} - A\right], \quad \frac{\overline{\Theta}_\infty}{\theta_*} = \frac{1}{k_\theta}\left[\ln\frac{u_*\delta}{\nu} - C\right], \tag{12), (13}$$

where k and k_θ are von Kármán constants for the surface-layer velocity and temperature profiles, respectively, and A and C are universal constants. Equations (12) and (13) can also be expressed in terms of the friction coefficient $C_f = (u_*/\overline{U}_\infty)^2$ and Stanton number $St \equiv -Q_0/\overline{U}_\infty\overline{\Theta}_\infty = u_*\theta_*/\overline{U}_\infty\overline{\Theta}_\infty$. The same drag and heat-transfer relations can be used for the stratified boundary layer also, provided that A and C are now considered as functions of the bulk stability parameter Ri_δ. Such a simple extension was originally proposed by Zilitinkevich, Laikhtman & Monin (1967) for the atmospheric boundary layer and has come to be widely accepted by meteorologists (see, for example, Arya 1975).

3. Wind tunnel and instrumentation

The wind tunnel used for experiments reported here has been described in detail by Plate & Cermak (1963). The closed-circuit tunnel has a $1{\cdot}8 \times 1{\cdot}8 \times 28$ m long test section. After an initial 12·2 m wooden section the floor consists of an equal length of aluminium plate which can be cooled or heated to any desired temperature between -5 and 200 °C. The air-conditioning system allows the ambient air temperature to be maintained anywhere between 5 and 65 °C.

Mean velocities were measured using a standard Pitot-static tube, whose output to a differential pressure transducer was integrated and averaged over a period of 4 min. Temperatures were simultaneously measured point by point with a copper–constantan thermocouple. Plate temperatures were monitored by a set of thermocouples embedded in the aluminium plate at 30 cm intervals along the centre-line. Velocity and temperature fluctuations were measured by three fine hot wires (one operated in the normal and two in the X-configuration) and a cold wire operated as a resistance thermometer. The hot wires were sensitive to velocity as well as temperature fluctuations and an elaborate calibration and measurement technique (for details see Arya & Plate 1969*a*) was employed to obtain all turbulent intensities and fluxes of interest, within estimated errors of ± 10 % and ± 15 %, respectively. Detailed turbulence measurements were made only for the stably stratified (cold plate) cases. For these, the wall shear stress τ_0 and the wall heat flux Q_0 were inferred from turbulent flux measurements at several heights close to the surface, which indicated a constant-flux layer (see Arya & Plate 1969*b*). For unstable conditions, Q_0 was estimated from the electric power supplied to the plate heaters after accounting for some radiation and conduction losses (Arya 1972*b*), and τ_0 or u_* was obtained by using the so-called 'profile' method, which was modified to include buoyancy effects.

4. Results and discussion

After the hot or cold air entered the test section, a constant-pressure boundary layer developed along the tunnel floor (the tunnel ceiling was adjusted to obtain a zero pressure gradient). The boundary layer was artificially tripped by a saw-tooth fence at the entrance and somewhat thickened by 1·2 cm gravel roughness placed on the initial 2 m length of the floor. Measurements were made at two stations A and B located respectively at 21·4 and 23·8 m from the entrance.

Stability group	Station	$\overline{U}_\infty$ (cm/s)	$\overline{\Theta}_\infty$ (°C)	δ (cm)	δ_θ (cm)	$\frac{u_*}{\overline{U}_\infty}$	$\frac{\theta_*}{\overline{\Theta}_\infty}$	$Re_\delta \times 10^{-5}$	Ri_δ
I	*B*	310	41·7	73	58	0·024	0·019	1·1	0·098
	B	306	39·5	73	57	0·024	0·019	1·1	0·099
II	*A*	604	42·8	66	55	0·031	0·024	1·9	0·024
	B	607	43·3	70	56	0·030	0·023	2·0	0·026
III	*A*	918	42·6	65	55	0·035	0·030	2·9	0·010
	B	912	42·2	68	59	0·035	0·029	3·0	0·011
IV	*B*	311	0	78	0	0·038	—	1·3	0
	B	922	0	70	0	0·036	—	3·5	0
V	*A*	619	−118	52	52	0·041	0·058	1·9	−0·050
	A	612	−123	51	51	0·040	0·057	2·0	−0·053
VI	*A*	459	−135	54	54	0·044	0·062	1·5	−0·120
	A	456	−133	54	54	0·045	0·063	1·5	−0·121
VII	*A*	306	−151	60	60	0·053	0·066	1·1	−0·324
	A	305	−150	60	60	0·054	0·067	1·1	−0·326

TABLE 1. Boundary-layer parameters

Table 1 gives all the essential boundary-layer parameters for the various runs, which are divided into 7 stability groups, depending on the value of Ri_δ.

Mean velocity and temperature profiles

Velocity and temperature profiles for the wall region ($z/\delta \lesssim 0{\cdot}15$) are presented in figures 1 (*a*) and (*b*). They appear curved mainly because of buoyancy effects; their curvature depends on the stability parameter ζ. Close to the surface (but well above the viscous sublayer), the profiles approach the expected logarithmic form

$$\frac{\overline{U}}{u_*} = \frac{1}{k}\ln\frac{u_* z}{\nu} + B, \quad \frac{\overline{\Theta}}{\theta_*} = \frac{1}{k_\theta}\ln\frac{u_* z}{\nu} + B_\theta, \tag{14), (15}$$

in which we find for the slightly stable or near-neutral runs (group III) $k_\theta \simeq k = 0{\cdot}41$, and B and B_θ depend on the stability.

The value of B is related to the thickness δ_ν of the viscous sublayer. For example, according to Rotta's theory (see Hinze 1959, p. 477),

$$B = k^{-1}\ln(4k-1) + u_*\delta_\nu/\nu. \tag{16}$$

Similarly, B_θ may also be related to the thickness of the thermal sublayer, in which heat is transferred mainly through conduction. The mean velocity profiles very close to the surface were used to determine B and then, from (16), $u_*\delta_\nu/\nu$ for each stability group. For the stable groups III, II and I, the values are 6·1, 8·5 and 11·1, respectively. The increase in the sublayer thickness with increasing stratification is probably caused by the stabilizing effect of buoyancy, which suppresses turbulence more effectively than viscosity alone would do. For unstable conditions, by the same reasoning, one might expect some thinning of the viscous sublayer with increasing instability. Our observations do not indicate this trend to be very significant, however. Close to the surface (say, for

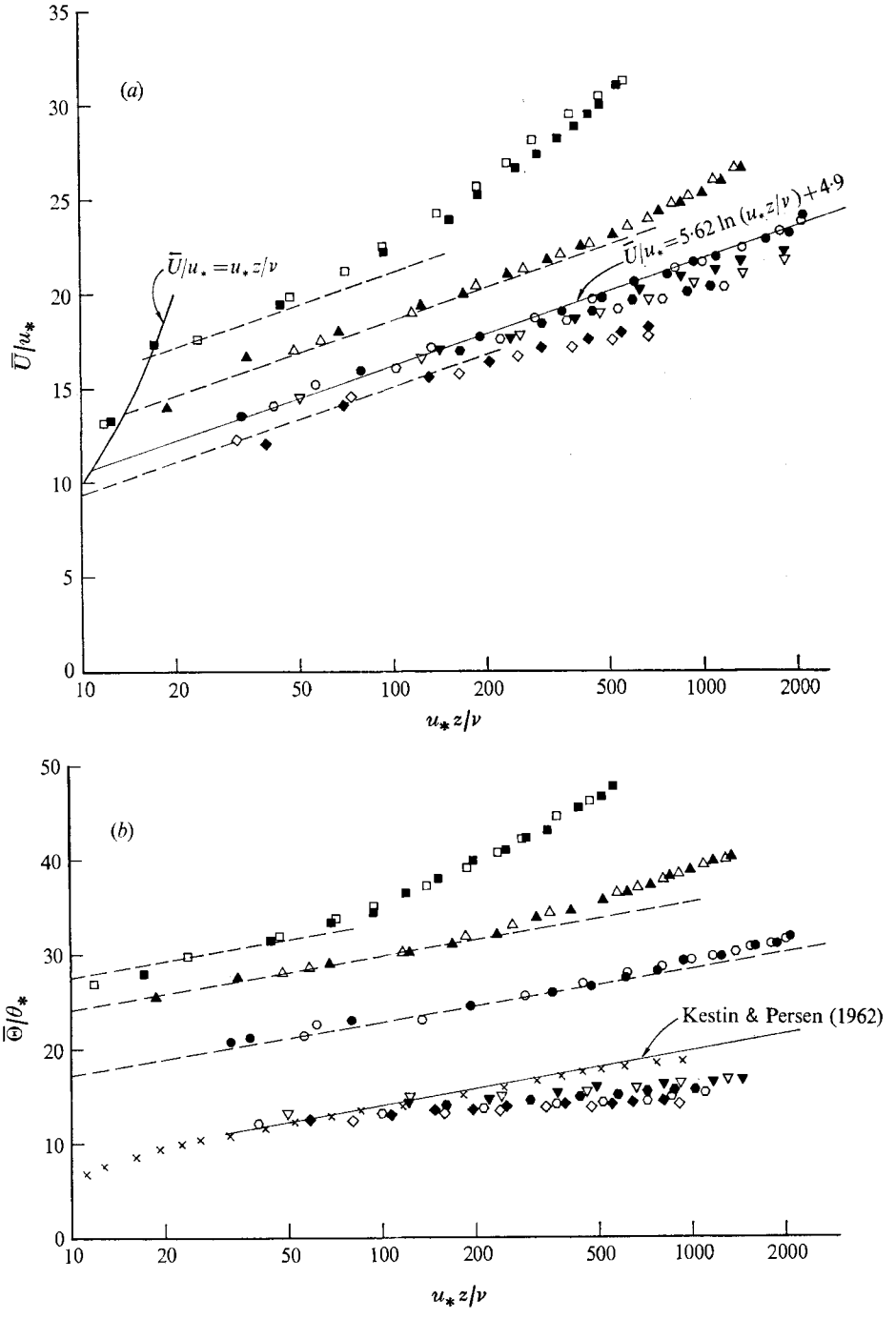

FIGURE 1. Surface-layer similarity profiles of (*a*) mean velocity and (*b*) temperature. ×, Blom (1970), group IV.

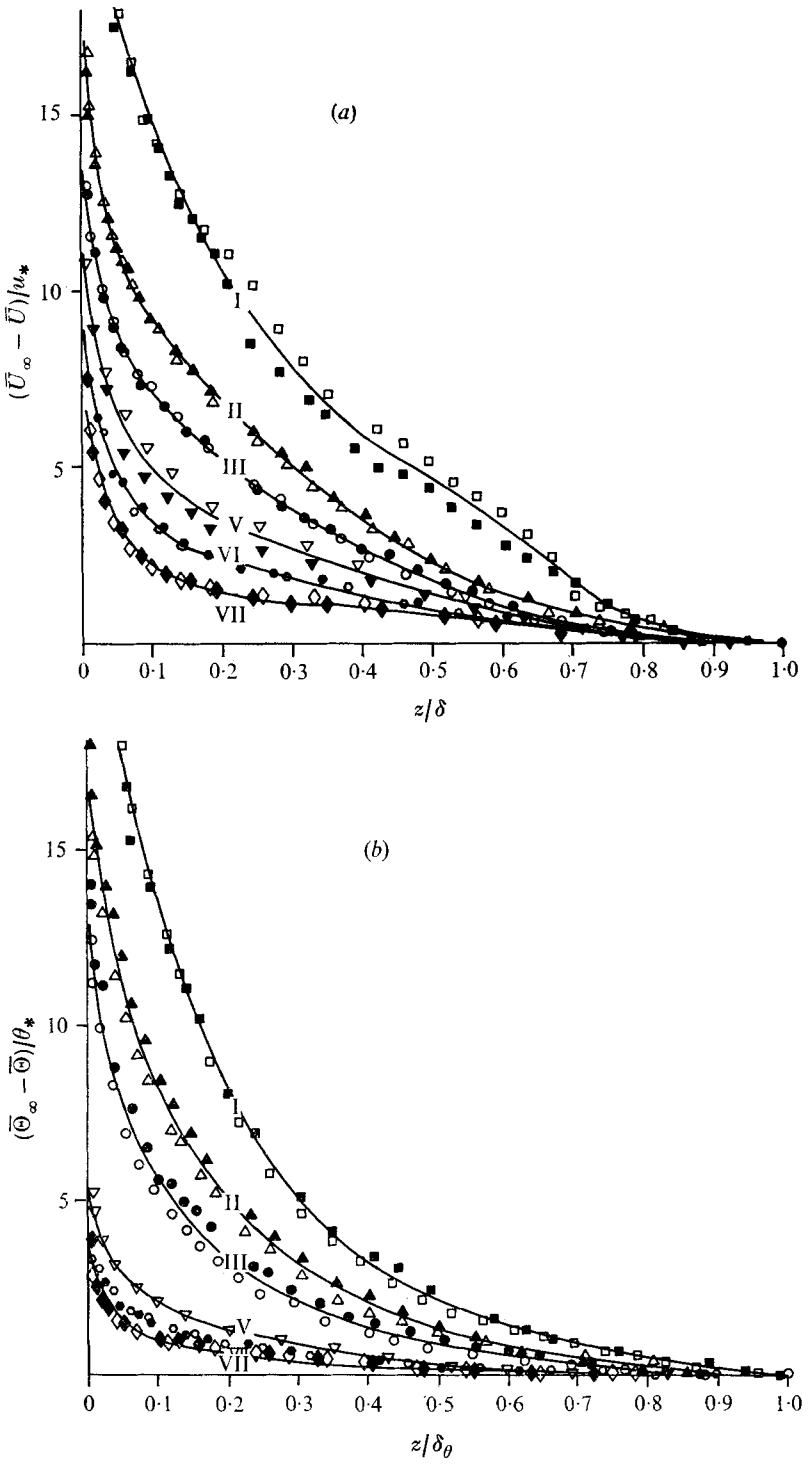

FIGURE 2. (*a*) Velocity- and (*b*) temperature-defect profiles for various stability groups.

Stability group	I	II	III	V	VI	VII
Ri_δ	0·099	0·025	0·011	−0·052	−0·121	−0·325

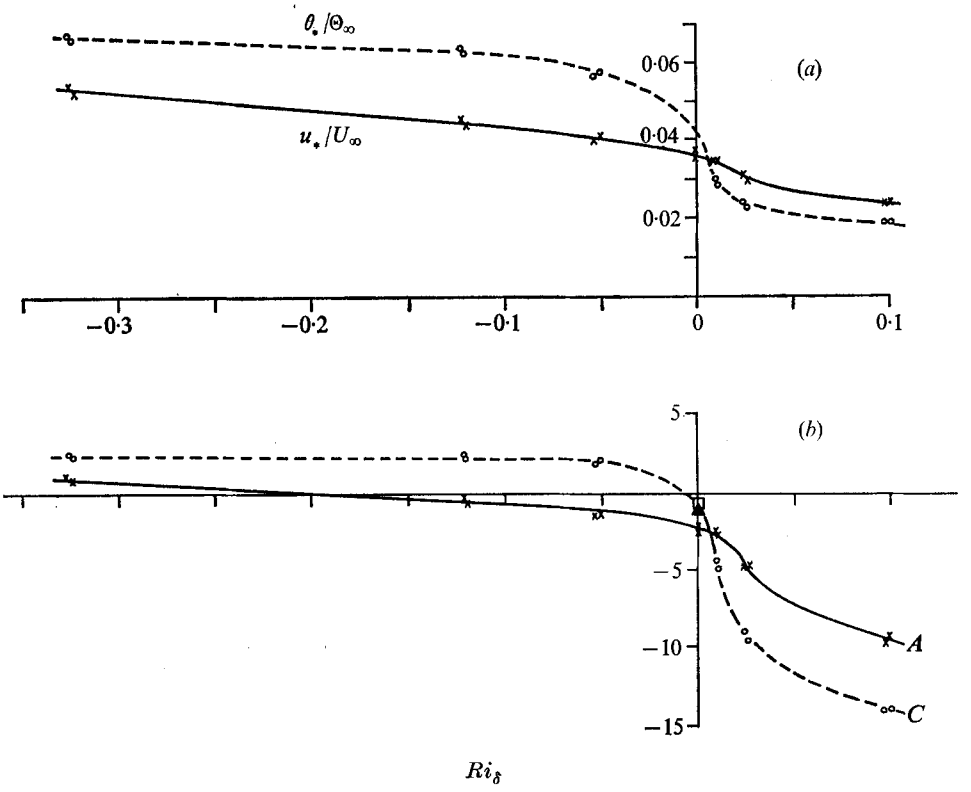

FIGURE 3. The effect of buoyancy on the friction and heat-transfer relations. (*a*) The ratios $u_*/\overline{U}_\infty$ and $\theta_*/\overline{\Theta}_\infty$ as functions of Ri_δ. (*b*) A and C in (12) and (13) as functions of Ri_δ. C: □, Blom (1970); ▲, Brundrett & Burroughs (1967); ○, present study. A: ×, present study.

$u_* z/\nu \lesssim 120$), but in the fully developed turbulent region, all the unstable velocity profiles in groups V and VI approach the universal logarithmic form for neutral boundary layers with $B \simeq 4{\cdot}9$ (Clauser 1956) and $u_* \delta_v/\nu \simeq 11{\cdot}1$, but those in group VII indicate a slightly thinner sublayer. All the unstable temperature profiles approach closely those measured or otherwise calculated for the near-neutral (slightly heated plate) case (Kestin & Persen 1962; Brundrett & Burroughs 1967; Blom 1970).

The velocity and temperature distributions in the outer region of our stratified boundary layer are shown in figures 2(*a*) and (*b*) in the usual 'defect' form. In this way any variation with Reynolds number is expected to be eliminated, especially within the narrow range of Re_δ in our experiments (see Clauser 1956). Large variations in the defect profiles in figure 2 are, therefore, mainly due to changes in thermal stratification. The velocity and temperature defects become very small under unstable conditions because of the enhanced mixing due to buoyancy, and the determination of the boundary-layer thickness becomes more uncertain (see Arya 1972*b*).

The effect of buoyancy on the friction and heat-transfer relations is shown in figures 3(*a*) and (*b*); both $u_*/\overline{U}_\infty$ and $\theta_*/\overline{\Theta}_\infty$ decrease with increasing stability.

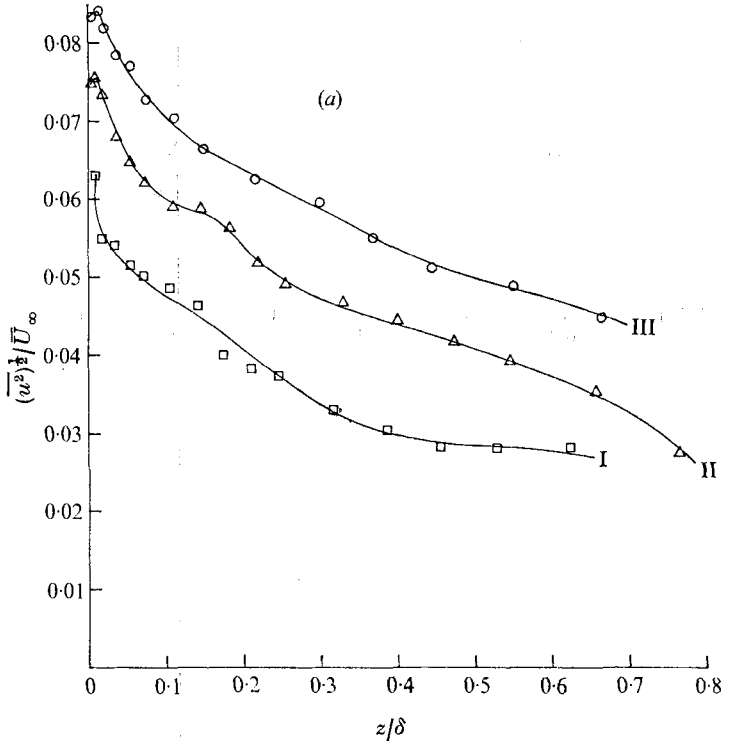

FIGURE 4(*a*). For legend see next page.

Much of the apparent variation on the unstable side is actually associated with the decreasing values of Re_δ associated with increasing instability. The effect of buoyancy alone on the friction and heat-transfer relations is better seen from the plot of A and C of (12) and (13) against Ri_δ given in figure 3(*b*). Here, the values of C in neutral conditions ($Ri_\delta \approx 0$) are taken from observations by Brundrett & Burroughs (1967) and Blom (1970). The variation of A and C with stability is similar to that observed for the atmospheric boundary layer (Arya 1975), although strict correspondence between the two cases is not warranted owing to the presence of Coriolis effects in the latter. One also encounters a much larger range of Ri_δ in the atmosphere than it has been possible to obtain in the laboratory.

Turbulence structure

Except for the r.m.s. temperature fluctuations, which were measured for both stable and unstable conditions, other measurements of turbulence are only available for the stable and neutral groups I–IV. The r.m.s. velocity fluctuations normalized by the ambient velocity are given in figures 4(*a*)–(*c*). According to the similarity hypothesis discussed earlier, their distributions with the normalized height z/δ must show the effects of changes in both Re_δ and Ri_δ. Unfortunately these two parameters could not be varied independently in our experiments and higher magnitudes of Ri_δ are associated with lower Re_δ. In order to show the effects of buoyancy alone, some data have been presented for neutral conditions

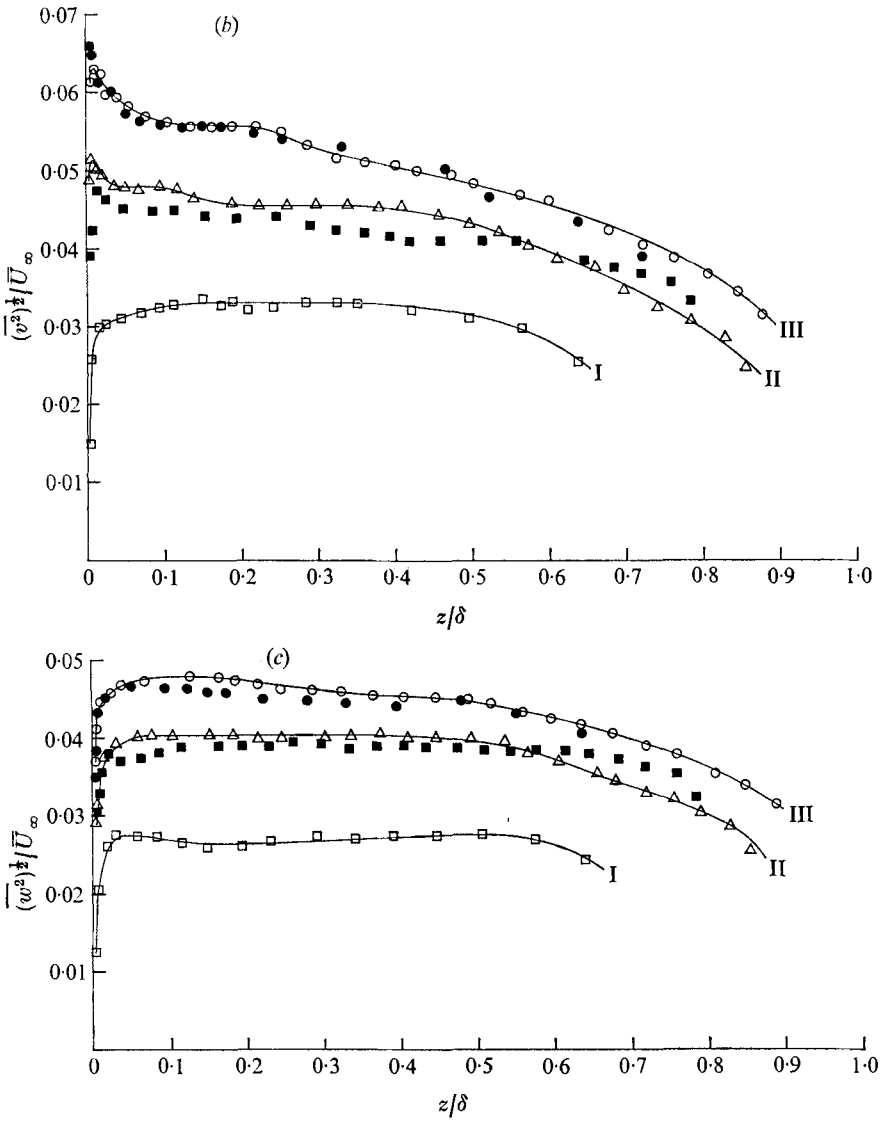

FIGURE 4. Distributions of r.m.s. fluctuations in (*a*) longitudinal, (*b*) lateral and (*c*) vertical velocity under stable and neutral conditions.

	□	△	○	●	■
Stability group	I	II	III	IV	IV
Ri_δ	0·099	0·025	0·011	0	0
$Re_\delta \times 10^{-5}$	1·1	2·0	3·0	3·5	1·3

(group IV) for the same Re_δ. Figures 4(*b*) and (*c*) indicate that, although some of the reduction in fluctuation intensities is caused by the decrease in Re_δ, the increase in stability results in a larger reduction in turbulence.

The mechanism by which the buoyancy reduces turbulence in stably stratified shear flows has been explained by Stewart (1959) and Lumley & Panofsky (1964, p. 73). Buoyancy forces extract energy directly only from the vertical component

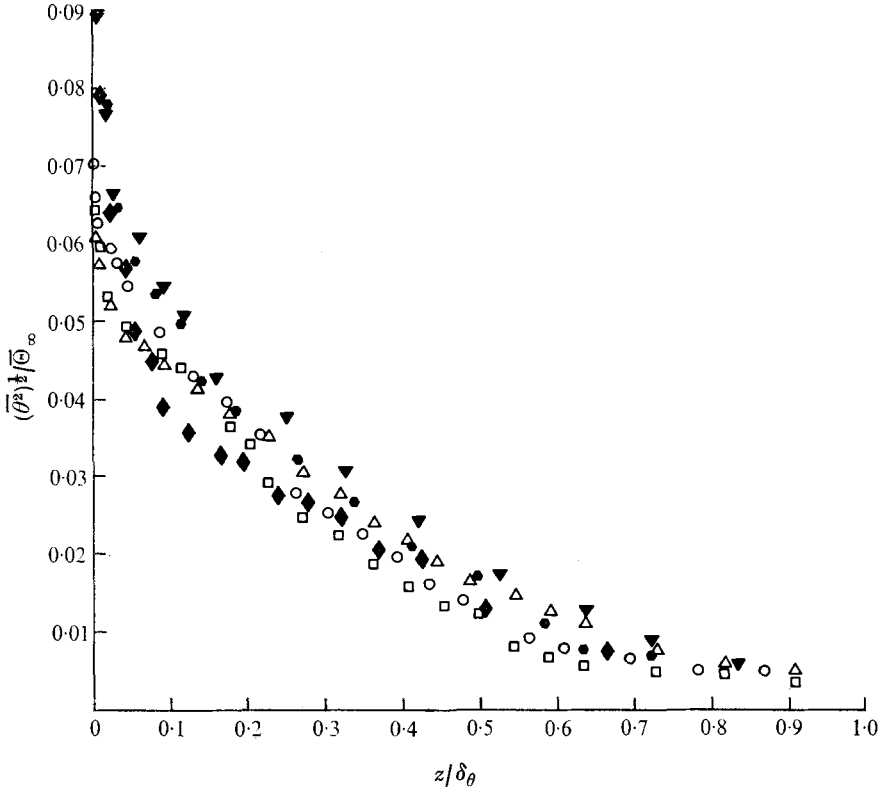

FIGURE 5. Distribution of r.m.s. fluctuations in temperature under stable and unstable conditions. Symbols as in figure 2.

of the velocity, thereby reducing $\overline{w^2}$, and also $-\overline{uw}$. As in neutral boundary layers, the interaction of $\overline{uw}$ with the mean velocity gradient contributes directly only to the u component, whence the energy is redistributed to the v and w components by the action of pressure fluctuations. In the layer near the surface in which most of the total energy production occurs, the velocity gradient has been shown to decrease with increasing stability for the same u_* (see figure 3). The extraction of energy by buoyancy, on the other hand, increases with increasing stability. This results in the suppression of all three components and not just the vertical component. The above reasoning also explains why the ratio $\overline{w^2}/\overline{u^2}$ remains relatively unaffected by stability.

In contrast to the velocity fluctuations, the intensity $(\overline{\theta^2})^{\frac{1}{2}}\,\overline{\Theta}_\infty$ of temperature fluctuations is seen to be very little affected by stratification (figure 5). Fluctuations in temperature occur as a consequence of the fluctuations in velocity. It is not quite clear why the former should simply be scaled by the temperature differential $\overline{\Theta}_\infty$ and remain more or less independent of the ambient velocity. The same behaviour is indicated by our temperature measurements in unstable conditions, which are also given in figure 5. In spite of the very large temperature differentials ($\overline{\Theta}_\infty = -118$ to $-151\,^\circ$C) for these unstable runs $(\overline{\theta^2})^{\frac{1}{2}}/\overline{\Theta}_\infty$ *vs.* z/δ_θ distributions are not much different from those under stable conditions.

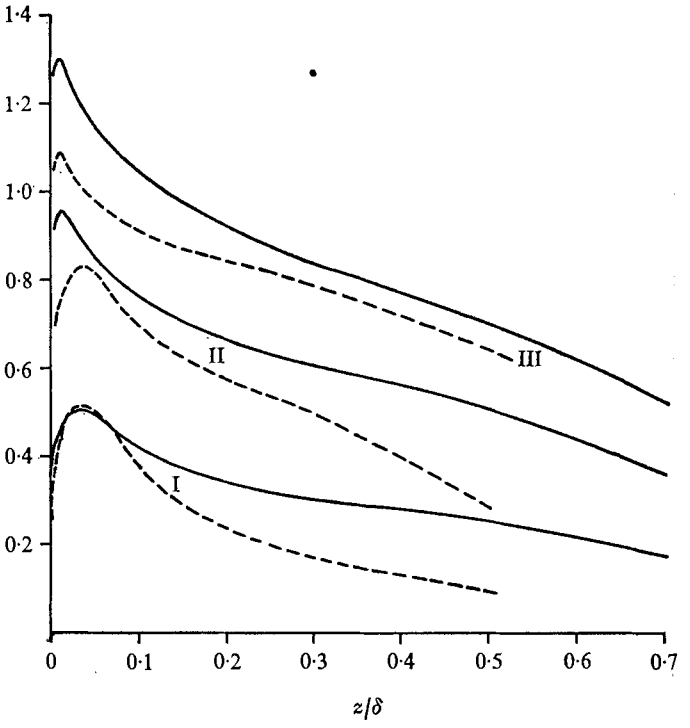

FIGURE 6. Distributions of the turbulent energy and momentum flux under stable conditions. ——, $(q^2/\overline{U}_\infty^2) \times 10^2$; – – –, $(-\overline{uw}/\overline{U}_\infty^2) \times 10^3$.

In figure 6 measured distributions of turbulent energy $q^2 = \overline{u^2}+\overline{v^2}+\overline{w^2}$ and shear stress in the boundary layer for three stability conditions are shown. Apparently, buoyancy affects shear stress more than it affects turbulent energy. In the outer region, the ratio $-\overline{uw}/q^2$, which is an important parameter in certain analytical formulations (Bradshaw 1967), decreases with increasing stability (typical values for groups III, II and I are 0·009, 0·007 and 0·004, respectively).

Of special significance are the fluxes of heat in the vertical and the horizontal directions (figure 7). Compared with $-\overline{w\theta}$, the horizontal flux $\overline{u\theta}$ decreases much faster with distance from the wall and its normalized values appear to be less affected by stability. A more surprising result is that, in the near-wall region, $\overline{u\theta}$ is several times $-\overline{w\theta}$, and their ratio $-\overline{u\theta}/\overline{w\theta}$ increases with increasing stability. This is in general agreement with observations in the surface layer of the atmosphere (Zubkovski & Tsvang 1966; Weseley, Thurtell & Tanner 1970; Wyngaard *et al.* 1971).

Why the horizontal heat flux should be much greater than the vertical flux in a homogeneous layer is not so obvious. If the relative magnitudes of the production terms in their dynamical equations are, in some way, indicative of the relative magnitude of the fluxes themselves, one may reason that, while $-\overline{w\theta}$ is produced by only one term, $\overline{w^2}\,\partial\overline{\Theta}/\partial z$, $\overline{u\theta}$ is produced by two terms, $-\overline{uw}\,\partial\overline{\Theta}/\partial z$ and

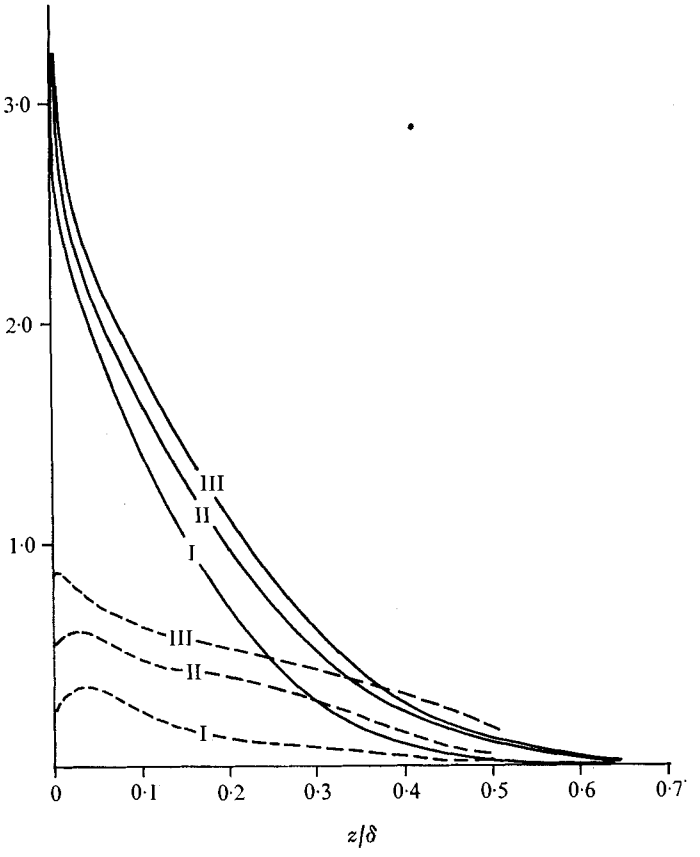

FIGURE 7. Distributions of the horizontal and vertical heat fluxes under stable conditions. ——, $(\overline{u\theta}/\overline{U}_\infty\overline{\Theta}_\infty)\times 10^3$; – – –, $(-\overline{w\theta}/\overline{U}_\infty\overline{\Theta}_\infty)\times 10^3$.

$-\overline{w\theta}\,\partial\overline{U}/\partial z$, of comparable magnitude. Another way of looking at the fluxes is through their correlation coefficients

$$\gamma_{u\theta}=\overline{u\theta}/(\overline{u^2})^{\frac{1}{2}}(\overline{\theta^2})^{\frac{1}{2}} \quad \text{and} \quad \gamma_{w\theta}=\overline{w\theta}/(\overline{w^2})^{\frac{1}{2}}(\overline{\theta^2})^{\frac{1}{2}}.$$

Figure 8 shows that, although $\gamma_{u\theta}$ decreases rapidly away from the surface, it has surprisingly large values in the surface layer. A similar conclusion can be drawn from the observations presented by Nicholl (1970).

A very plausible explanation for the high correlation between u and θ is that both are produced by vertical movements through the mean gradients (Webb 1970). In the region close to the wall where mean gradients are large (but not so close that the vertical velocity is diminished by the wall effects), the dominant terms in the equations for u and θ are $-w\,\partial\overline{U}/\partial z$ and $-w\,\partial\overline{\Theta}/\partial z$, respectively, which are quite similar. Thus, any negative w produces a positive u and θ and vice versa. Only the fact that the fluctuating pressure-gradient term is present in the u equation and not in the θ equation prevents the correlation from becoming essentially unity. The w equation, on the other hand, has no mean gradient term, but has a buoyancy destruction term (which is absent from both the u and θ equations). Thus there is less similarity between this equation and the θ equation

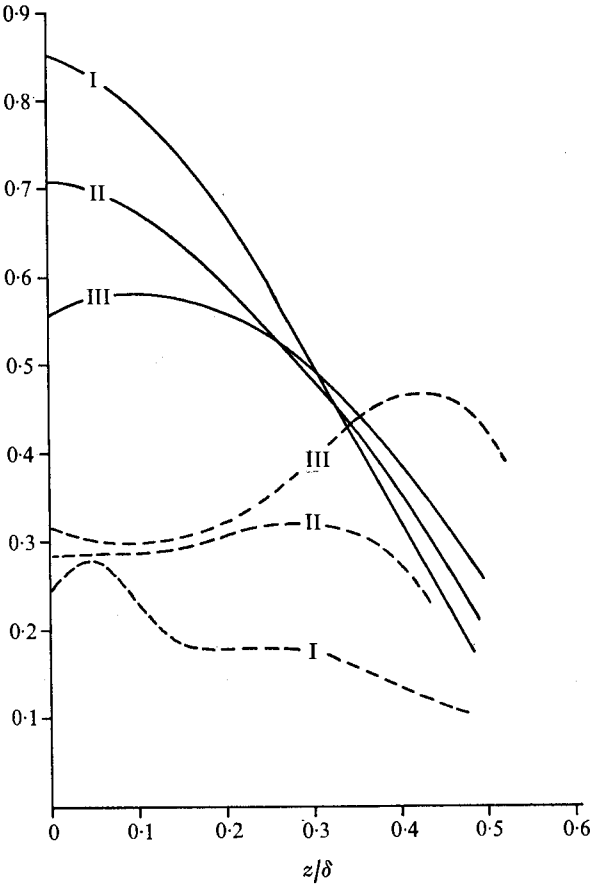

FIGURE 8. Distributions of the correlation coefficient of the horizontal and vertical heat fluxes under stable conditions. ——, $\gamma_{u\theta}$; – – –, $-\gamma_{w\theta}$.

than between the u and θ equations. Therefore, θ and w are not as highly correlated as θ and u.

The correlation coefficient $-\gamma_{w\theta}$ is seen to decrease in magnitude with increasing stability (figure 8), indicating the hampering effect of stable stratification on the transfer of heat in the vertical. The corresponding effect on momentum transfer is less and mostly limited to the outer layer (figure 9). Also plotted in figure 9 is the ratio ϵ_h/ϵ_m of the eddy exchange coefficients of heat and momentum, which is a measure of the relative transfer of heat and momentum. Heat-transfer studies indicate that the average value of ϵ_h/ϵ_m in a near-neutral boundary layer is close to unity. Actually, it has been observed to vary somewhat with the distance from the surface; close to the surface, a value of about 1·3 is more appropriate (Blom 1970). About the same value has been found for the near-ground layer of the atmosphere in near-neutral conditions (Businger *et al.* 1971).

Atmospheric observations under stable conditions do not indicate any significant change in ϵ_h/ϵ_m with stability (Webb 1970; Businger *et al.* 1971) although there are some exceptions (Carl, Tarbell & Panofsky 1973). Laboratory data, on the other hand, show a significant decrease in ϵ_h/ϵ_m with increasing

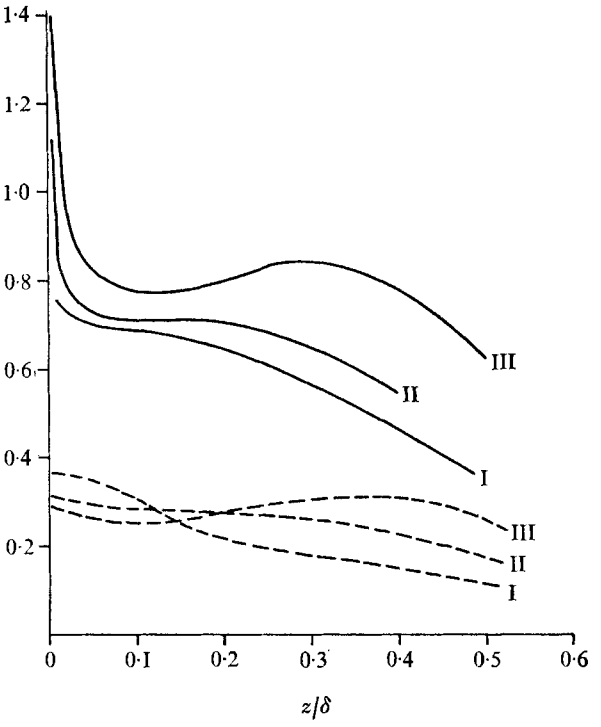

FIGURE 9. Distributions of the correlation coefficient of momentum flux and the ratio of the eddy exchange coefficients of heat and momentum under stable conditions. ——, ϵ_h/ϵ_m; – – –, $-\gamma_{uw}$.

stability (Ellison & Turner 1960; Arya & Plate 1969*b*). A probable explanation for this difference is that in the laboratory more stable conditions have become associated with such low Reynolds numbers that the Reynolds number effect can no longer be neglected. Another reason might be that, in the laboratory flows, the fluxes varied too much even in the assumed surface layers. Horizontal homogeneity and constancy of fluxes are better realized in the surface layer of the atmosphere, where ϵ_h/ϵ_m is found to remain almost constant in stable conditions. There is no evidence, however, that this is also true for the flow in the outer layer (see, for example, Carl *et al.* 1973). From our experiments flux measurements are available only for the lower half of the boundary layer, in which ϵ_h/ϵ_m depends on $z/\delta Ri_\delta$ and possibly also on Re_δ. The individual effects of Ri_δ and Re_δ cannot be separated out. There is, unfortunately, no study on the effect of Reynolds number on ϵ_h/ϵ_m in near-neutral conditions. Reported measurements of ϵ_h/ϵ_m in the heat-transfer literature are so few and often so conflicting that it is even difficult to make out from these whether ϵ_h/ϵ_m decreases or increases with distance from the wall (see, for example, Blom 1970).

Plotted in figure 10 are the distributions of the flux and stress Richardson numbers, defined as

$$R_f = \frac{g}{T_0}\frac{\overline{w\theta}}{\overline{uw}}\frac{\partial \overline{U}}{\partial z}, \quad R_s = \frac{g}{T_0}\frac{\overline{w\theta}}{\overline{w^2}}\frac{\partial \overline{U}}{\partial z}. \tag{17}$$

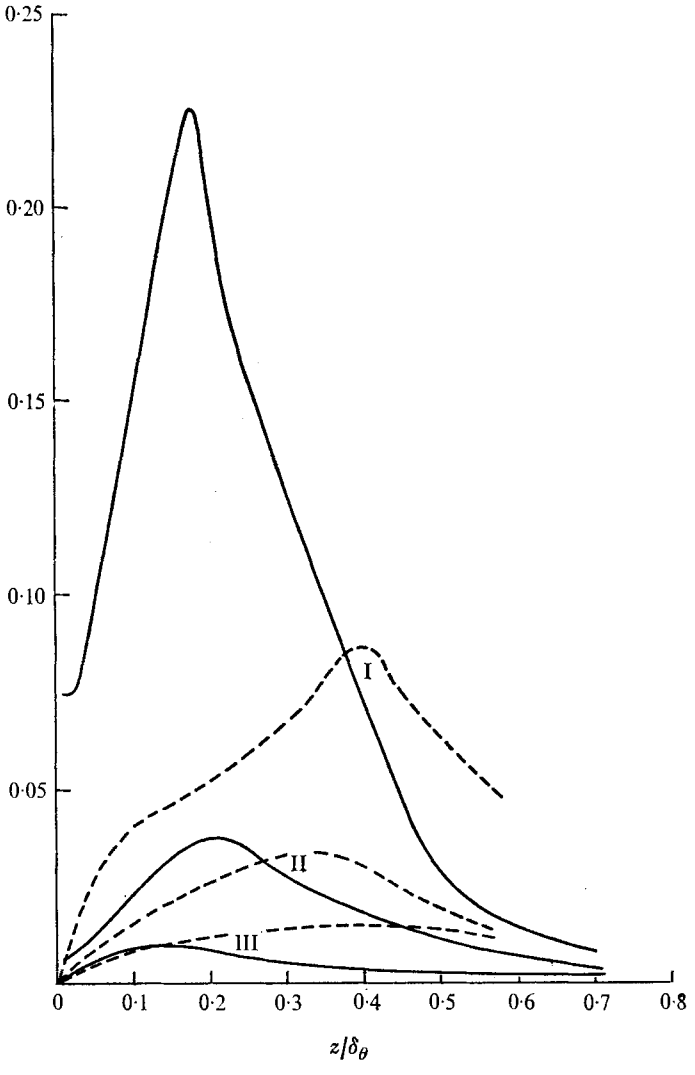

FIGURE 10. Distributions of the flux and stress Richardson numbers for stability groups I, II and III. ——, R_s; – – –, R_f.

They represent the ratio of buoyancy destruction to the mechanical production terms in the budget equations for q^2 and $-\overline{uw}$, respectively. The peak in R_s occurs within or near the top of the surface layer and well below the level of the maximum in R_f. Here, the ratio R_s/R_f seems to increase very rapidly with increasing stability, indicating that, in a stably stratified surface layer, buoyancy plays a more dominant role in the stress budget than it does in the turbulent energy budget. This was also stressed earlier by the author while proposing a simple model for predicting the critical Richardson number (Arya 1972*a*). The critical condition was not approached, however, in the laboratory experiments described here.

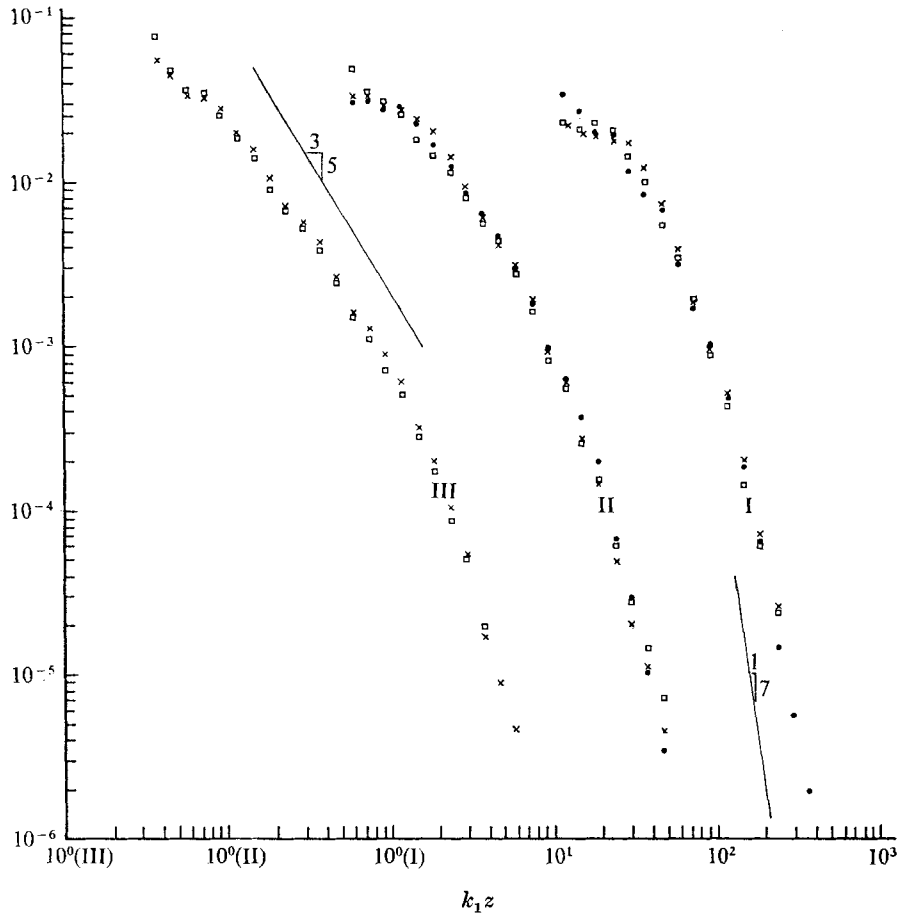

FIGURE 11. Spectra of the lateral and vertical velocity and temperature fluctuations at 25 cm above the surface for stability groups I, II and III. □, $\phi_v(k_1)/\overline{v^2}$; ×, $\phi_w(k_1)/\overline{w^2}$; ●, $\phi_\theta(k_1)/\overline{\theta^2}$.

In order to study the effect of buoyancy on eddy sizes we have measured the spectra of v, w and θ; these are plotted in figure 11 in normalized form for three stability conditions. The relative height z/δ is about the same for all spectra. Note that the spectral shapes for v, w and θ are very similar. This was also observed earlier by Plate & Arya (1969) for the wall region. The range of wave-numbers in which the spectrum of any of the quantities can be approximated by the $-\frac{5}{3}$-power law (inertial subrange) decreases considerably with increasing stability. Part of the effect is of course due to the reduction in Re_δ, since the Reynolds number largely determines the range of eddy sizes to be expected.

It has been argued by Bradshaw (1967) that small eddy motion including that in the dissipation range is a function only of the local shear stress $-\overline{uw}$ and the thickness δ of the boundary layer. This gives $(-\overline{uw})^{\frac{1}{2}}$ and δ as the appropriate velocity and length scales. One expects, then, that in the so-called equilibrium range spectra of any of the components of the velocity fluctuations measured at

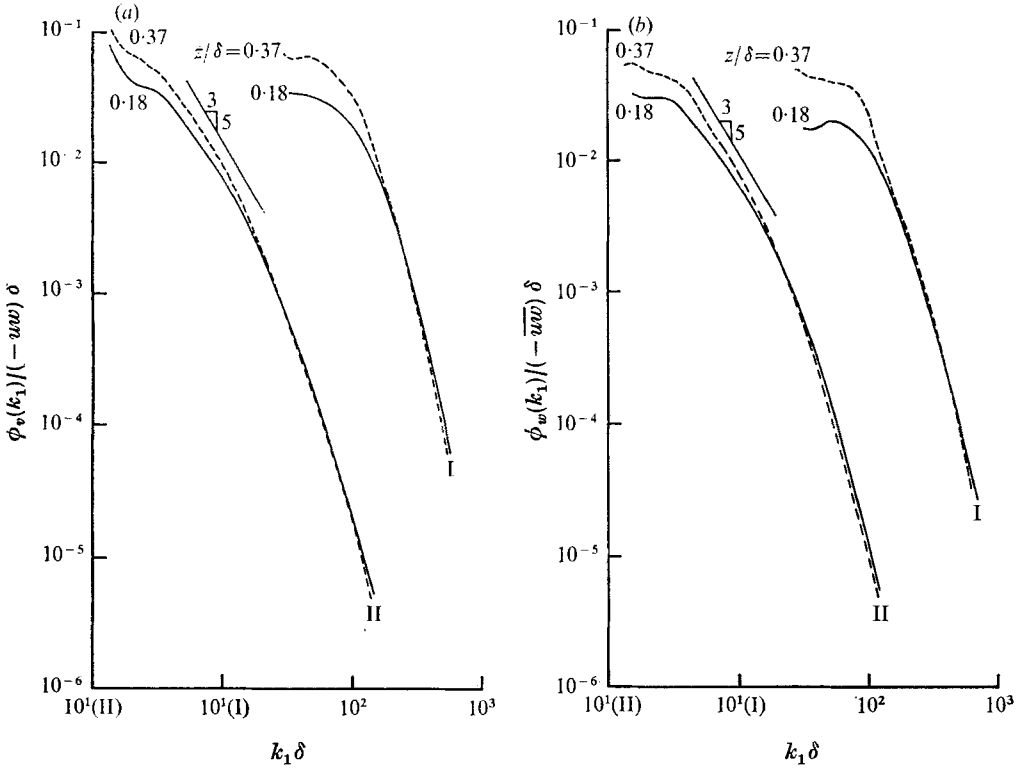

FIGURE 12. Similarity spectra of (*a*) lateral and (*b*) vertical velocity fluctuations at two positions in the boundary layer for stability groups I and II.

different heights in the boundary layer collapse together when normalized with the above scales. Although our observations do not extend very far out in the outer layer, figures 12(*a*) and (*b*) do support this similarity hypothesis. Normalization by mean-square fluctuations was found to be less satisfactory and has not been shown here.

A similar collapse of temperature spectra would be expected if these were normalized by a temperature scale $-\overline{w\theta}/(-\overline{uw})^{\frac{1}{2}}$ and δ_θ. After some comparisons, however, we found that this choice of scales is no better than that of $(\overline{\theta^2})^{\frac{1}{2}}$ and δ or δ_θ, and the collapse in both the cases is less satisfactory (figure 13).

Several studies have been made in the past of the effect of buoyancy on the spectra of turbulence in stably stratified flows (Bolgiano 1959; Lumley 1964). Of special interest has been the spectral behaviour in the so-called buoyant subrange, for which it is stipulated that the mechanical production is not as significant as the energy extraction by buoyancy. In spite of the differences in the details of the various models, these generally agree that in this subrange the spectrum of w is steeper and that of θ flatter than the $-\frac{5}{3}$-power law for the inertial subrange (see Phillips 1967). Lumley (1967) has discussed the criteria for the existence of a buoyant subrange. Since the conflicting requirements of large Reynolds number and very strong stratification are not satisfied in our experiment, no buoyant-subrange behaviour is expected in the observed spectra.

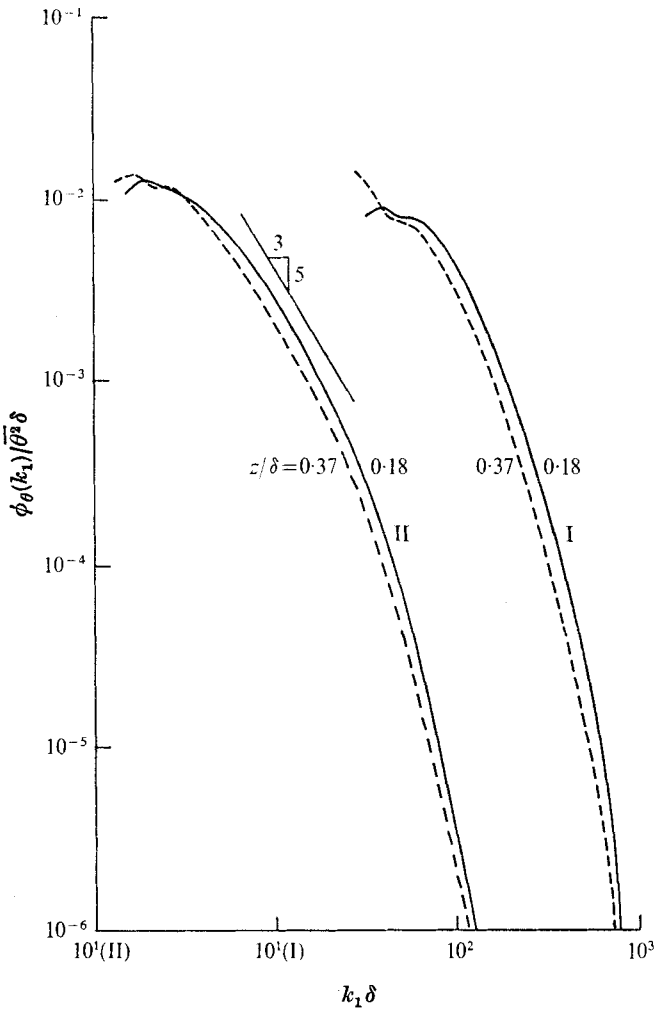

FIGURE 13. Similarity spectra of temperature fluctuations at two positions in the boundary layer for stability groups I and II.

The wavenumber corresponding to the peak energy, however, increases with increasing stability, a trend also observed in the atmospheric spectra (Monin 1962).

5. Conclusions

Buoyancy effects on the mean flow and turbulent structure of a thermally stratified boundary layer developed on the floor of a long (28 m) wind-tunnel test section have been investigated. Observations taken for several stable and unstable stratifications have been discussed in a similarity framework derived from a simple extension of the concept of equilibrium boundary layers to stratified conditions. For the wall region, when $\overline{U}/u_*$ and $\overline{\Theta}/\theta_*$ are plotted against $\ln(u_* z/\nu)$,

their profiles appear not only curved, which is a well-known stability effect, but also displaced along the ordinate in a manner which suggests that the heights of the molecular sublayers of momentum and heat transfer are also affected by buoyancy.

In the outer region, the velocity- and temperature-defect profiles were shown to be strongly dependent on the bulk Richardson number, which is a measure of the buoyancy effects. Owing to enhanced mixing under unstable conditions, the defects in the bulk of the boundary layer become very small. The coefficients of friction and heat transfer (Stanton number) were observed to decrease with increasing stability; these were given as functions of the Reynolds number and bulk Richardson number.

Normalized turbulent intensities, fluxes and their correlation coefficients also depend strongly on stability. For most of these, buoyancy effects appear mixed with the smaller effect of changes in Reynolds number, which, in our experiments, became associated with the variations in the bulk Richardson number. Under stably stratified conditions, for which most turbulence measurements were made, turbulence was shown to be greatly suppressed with increasing stratification. The horizontal heat flux is several times the vertical heat flux and their ratio decreases with increasing distance from the surface. The ratio of the eddy diffusivities of heat and momentum was also found to decrease with height as well as with increasing stability. Distributions of flux and stress Richardson numbers indicate that in the surface layer buoyancy effects are more dominant in the momentum flux budget than in the turbulent energy budget.

Finally, turbulent spectra of velocity and temperature fluctuations were presented to investigate possible effects of buoyancy on eddy sizes. Much of the variation in the spectral shapes for different stability groups is probably associated with the change in Reynolds number. The wavenumber corresponding to the peak energy was, however, found to increase with stability, a trend expected from some theories and atmospheric observations. No buoyancy subrange could be detected in our spectra since the proper conditions for the existence of such a subrange were also not met. The similarity scaling suggested by Bradshaw (1967) was found to be effective in collapsing spectra for different heights in the boundary layer.

I should like to thank the referees for their several helpful suggestions which have been incorporated in the final manuscript. Thanks are also due to Mrs Jo Ann Jarrett for typing the manuscript. The financial support for the original experimental work done at Colorado State University was provided by the U.S. Army Grant DA-AMC-28-043-65-G20. More recent support in writing up this paper has come from the National Science Foundation Grant GA 3317 XL.

REFERENCES

ARYA, S. P. S. 1968 Structure of stably stratified turbulent boundary layer. Ph.D. dissertation, Colorado State University, Fort Collins.

ARYA, S. P. S. 1972*a* The critical condition for the maintenance of turbulence in stratified flows. *Quart. J. Roy. Met. Soc.* **98**, 264–273.

ARYA, S. P. S. 1972*b* Free convection similarity and measurements in flows with and without shear. *J. Atmos. Sci.* **29**, 877–885.

ARYA, S. P. S. 1975 Geostrophic drag and heat transfer relations for the atmospheric boundary layer. *Quart. J. Roy. Met. Soc.* **101** (to appear).

ARYA, S. P. S. & PLATE, E. J. 1969*a* Hot-wire measurements in non-isothermal flow. *Instrum. & Control Syst.* **42**, 87–90.

ARYA, S. P. S. & PLATE, E. J. 1969*b* Modeling of the stably stratified atmospheric boundary layer. *J. Atmos. Sci.* **26**, 656–665.

BLOM, J. 1970 An experimental determination of the turbulent Prandtl number in a developing temperature boundary layer. Ph.D. dissertation, Technological University, Eindhoven, Netherlands.

BOLGIANO, R. 1959 Turbulent spectra in a stably stratified atmosphere. *J. Geophys. Res.* **64**, 2226–2229.

BRADSHAW, P. 1967 The turbulence structure of equilibrium boundary layers. *J. Fluid Mech.* **29**, 625–645.

BRUNDRETT, E. & BURROUGHS, P. R. 1967 The temperature inner-law and heat transfer for turbulent air flow in a vertical square duct. *Int. J. Heat Mass Transfer*, **10**, 1133–1142.

BUSINGER, J. A., WYNGAARD, J. C., IZUMI, Y. & BRADLEY, E. F. 1971 Flux profile relationships in the atmospheric surface layer. *J. Atmos. Sci.* **28**, 181–189.

CARL, D. M., TARBELL, T. C. & PANOFSKY, H. A. 1973 Profiles of wind and temperature from towers over homogeneous terrain. *J. Atmos. Sci.* **30**, 788–794.

CERMAK, J. E., SANDBORN, V. A., PLATE, E. J., BINDER, G. H., CHUANG, H., MERONEY, R. N. & ITO, S. 1966 Simulation of atmospheric motion by wind-tunnel flows. *Tech. Rep. Fluid Dyn. & Diffusion Lab., Colorado State University, Fort Collins*, no. 17.

CLAUSER, F. H. 1956 The turbulent boundary layer. *Adv. in Appl. Mech.* **4**, 1–51.

DEARDORFF, J. W. 1972 Numerical investigation of neutral and unstable planetary boundary layers. *J. Atmos. Sci.* **29**, 91–115.

DEARDORFF, J. W. & WILLIS, G. E. 1967 Investigation of turbulent thermal convection between horizontal plates. *J. Fluid Mech.* **28**, 675–704.

ELLISON, T. H. 1957 Turbulent transport of heat and momentum from an infinite rough plane. *J. Fluid Mech.* **2**, 456–466.

ELLISON, T. H. & TURNER, J. S. 1960 Mixing of dense fluid in a turbulent pipe flow. *J. Fluid Mech.* **8**, 514–544.

HINZE, J. O. 1959 *Turbulence.* McGraw-Hill.

KADER, B. A. & YAGLOM, A. M. 1972 Heat and mass transfer laws for fully turbulent wall flows. *Int. J. Heat Mass Transfer*, **15**, 2329–2353.

KESTIN, J. & PERSEN, L. N. 1962 Application of Schmidt's method to the calculation of Spalding function and of the skin-friction coefficient in turbulent flow. *Int. J. Heat Mass Transfer*, **5**, 143–152.

KRAUS, E. B. 1972 *Atmosphere–Ocean Interaction.* Oxford University Press.

LEWELLEN, W. S. & TESKE, M. 1973 Prediction of the Monin–Obukhov similarity functions from an invariant model of turbulence. *J. Atmos. Sci.* **30**, 1340–1345.

LUMLEY, J. L. 1964 The spectrum of nearly inertial turbulence in a stable stratified fluid. *J. Atmos. Sci.* **21**, 99–102.

LUMLEY, J. L. 1967 Theoretical aspects of research in turbulence in stratified flows. In *Atmospheric Turbulence and Radiowave Propagation*, pp. 105–110. Moscow: Nauka.

LUMLEY, J. L. & PANOFSKY, H. A. 1964 *The Structure of Atmospheric Turbulence.* Interscience.

MELLOR, G. L. 1973 Analytic prediction of the properties of stratified planetary surface layers. *J. Atmos. Sci.* **30**, 1061–1069.

MERY, P., SCHON, J. P & SOLAL, J. 1974 Comparison of thermally neutral and unstable shear flows in the wind tunnel and the atmosphere. *Adv. in Geophys.* B **18** (to appear).

MONIN, A. S. 1962 Empirical data on turbulence in the surface layer of the atmosphere. *J. Geophys. Res.* **67**, 3103–3109.

MONIN, A. S. 1965 On the symmetry properties in the surface layer of air. *Izv. Atmos. Oceanic Phys., Acad. Sci. U.S.S.R.* **1**, 25–30 (English trans.).

MONIN, A. S. & OBOUKHOV, A. M. 1954 Basic regularity in turbulent mixing in the surface layer of the atmosphere. *Trans. Geophys. Inst., Acad. Sci. U.S.S.R.*, no. 24 (151), pp. 163–187.

MONIN, A. S. & YAGLOM, A. M. 1971 *Statistical Fluid Mechanics: The Mechanics of Turbulence.* M.I.T. Press.

NICHOLL, C. H. I. 1970 Some dynamical effects of heat on a turbulent boundary layer. *J. Fluid Mech.* **40**, 361–384.

PHILLIPS, O. M. 1967 On the Bolgiano and Lumley–Shur theories of the buoyant subrange. In *Atmospheric Turbulence and Radiowave Propagation*, pp. 121–128. Moscow: Nauka.

PLATE, E. J. & ARYA, S. P. S. 1969 Turbulence spectra in a stably stratified boundary layer. *Radio Sci.* **4**, 1163–1168.

PLATE, E. J. & CERMAK, J. E. 1963 Micrometeorological wind tunnel facility: description and characteristics. *Fluid Dyn. & Diffusion Lab., Colorado State University, Fort Collins, Rep.* CER63EJP-JEC 9.

ROTTA, J. C. 1962 Turbulent boundary layers in incompressible flow. *Prog. Aero. Sci.* **2**, 1–219.

STEWART, R. W. 1959 The problem of diffusion in a stratified fluid. *Adv. in Geophys.* **6**, 303–311.

TOWNSEND, A. A. 1958 Turbulent flow in a stably stratified atmosphere. *J. Fluid Mech.* **5**, 361–372.

TURNER, J. S. 1973 *Buoyancy Effects in Fluids.* Cambridge University Press.

WEBB, E. K. 1970 Profile relationships: the log-linear range and extension to strong stability. *Quart. J. Roy. Met. Soc.* **96**, 67–90.

WESELEY, M. L., THURTELL, G. W. & TANNER, C. B. 1970 Eddy correlation measurements of sensible heat flux near the earth's surface. *J. Appl. Meteor.* **9**, 45–50.

WYNGAARD, J. C., COTÉ, O. R. & IZUMI, Y. 1971 Local free convection, similarity, and the budgets of shear stress and heat flux. *J. Atmos. Sci.* **28**, 1171–1182.

WYNGAARD, J. C., COTÉ, O. R. & RAO, K. S. 1974 Modeling of the atmospheric boundary layer. *Adv. in Geophys.* **A18** (to appear).

ZILITINKEVICH, S. S. & CHALIKOV, D. V. 1968 Determining the universal wind-velocity and temperature profiles in the atmospheric boundary layer. *Izv. Atmos. Ocean. Phys., Acad. Sci. U.S.S.R.* **4**, 165–169 (English trans.).

ZILITINKEVICH, S. S., LAIKHTMAN, D. L. & MONIN, A. S. 1967 Dynamics of the atmospheric boundary layer. *Izv. Atmos. Ocean. Phys., Acad. Sci. U.S.S.R.* **3**, 170–191 (English trans.).

ZUBKOVSKI, S. L. & TSVANG, L. R. 1966 Horizontal turbulent heat flow. *Izv. Atmos. Ocean. Phys., Acad. Sci. U.S.S.R.* **2**, 798–799 (English trans.).